



HAL
open science

DOMAIN WALL DYNAMICS IN ORTHORHOMBIC GARNETS

D. Krumbholz, J. Heidmann, J. Engemann

► **To cite this version:**

D. Krumbholz, J. Heidmann, J. Engemann. DOMAIN WALL DYNAMICS IN ORTHORHOMBIC GARNETS. Journal de Physique Colloques, 1985, 46 (C6), pp.C6-141-C6-144. 10.1051/jphyscol:1985625 . jpa-00224873

HAL Id: jpa-00224873

<https://hal.science/jpa-00224873>

Submitted on 4 Feb 2008

HAL is a multi-disciplinary open access archive for the deposit and dissemination of scientific research documents, whether they are published or not. The documents may come from teaching and research institutions in France or abroad, or from public or private research centers.

L'archive ouverte pluridisciplinaire **HAL**, est destinée au dépôt et à la diffusion de documents scientifiques de niveau recherche, publiés ou non, émanant des établissements d'enseignement et de recherche français ou étrangers, des laboratoires publics ou privés.

DOMAIN WALL DYNAMICS IN ORTHORHOMBIC GARNETS

D. Krumbholz, J. Heidmann and J. Engemann

University of Wuppertal, Dept. of Electrical Engineering, 5600 Wuppertal 1, F.R.G.

Résumé - Comme première investigation sur l'application de la mémoire à lignes de Bloch sur le grenat orthorhombique, comme proposé par Konishi, on a fait des simulations résolues en temps du mouvement de la paroi et des expériences dynamiques. Comme résultat principal, la nucléation des lignes de Bloch horizontales a été établie pour la première fois comme l'effet qui limite la vitesse. Puis on a examiné la dépendance de la vitesse maximale, par la nucléation des lignes de Bloch horizontales, sur l'épaisseur du film et sur la direction du mouvement relatif de la paroi par rapport à l'axe moyen.

Abstract - As a preliminary investigation for applying the Bloch line memory concept, as proposed by Konishi, to orthorhombic garnets, time resolved simulations of wall motion and dynamic experiments were carried out. As a main result, horizontal Bloch line nucleation was for the first time clearly established as the velocity limiting effect. Consequently the dependence of maximum velocity, due to horizontal Bloch line nucleation, on film thickness as well as on the direction of wall movement relative to the medium axis was examined.

I - INTRODUCTION

Extensive investigation of garnet films having orthorhombic anisotropy proves the general existence of two basic domain structures in materials of this class. Characteristic for the most elementary topological state is the uniform orientation of the central wall magnetization (Fig.1b), which parallels the medium axis of anisotropy (m.a.). The second basic state exhibits Bloch line structures, whereby the central wall magnetization is governed by the stray field (Fig.1a,c), resulting in a variety of wallstates most of which are metastable. The degree to which magnetostatic energy is minimized determines the particular Bloch line structure. The segmentation of stray field oriented areas in such domains can occur diversely owing to static stable horizontal and vertical Bloch line segments (HBL and VBL respectively). These Bloch line structures, characteristic for orthorhombic materials, will be designated by the following notation: $(S, nVBL/mHBL)^{+,-}$, where S indicates the net number of windings, n the quantity of VBL-segments, and m the quantity of HBL-segments. So far there is no experimental evidence of the stable existence of Bloch points. Given a comprehensive understanding of wall state characteristics in orthorhombic garnets /1,2/, inferences can be drawn about the mechanisms governing observed dynamic conversions. One necessary condition for the extension of Konishi's Bloch Line Memory (BLM) concept /3/ to orthorhombic garnets, the nucleation of horizontal Bloch lines, was demonstrated experimentally and in time resolved computer simulations. In order to achieve an improved quantitative comprehension of the dynamic Bloch line phenomena, time resolved computer simulations of the motion of a straight domain wall with and without HBL were conducted.

II - THEORY

As was already shown when limited to a steady state approximation /4/, the observed wall structures are part of the quantity of solutions of Slonczewski's equations of motion when extended by the orthorhombic anisotropy /5/. In addition, extended equations of motion were derived by employing Slonczewski's treatment, accompanied by the increased extension of the model used. Other extended versions were given by Hubert /6,7/. The coordinate system employed here is defined in /4/, as well as the notation used. Complementations to the notation are as follows: wall width $\Delta_0 = \sqrt{(A/K_u)}$, wall position q normalized to Δ_0 , z-coordinate normalized to film thickness h, Gilbert damping parameter α , gyromagnetic ratio γ and the pulse field h_p normalized on $4\pi M_s$. The examined extensions of the model make use of the description of an isolated planar wall under influence of an inplane field outlined in /1/. This model has been proved right when applied as description of all the wallstates' properties observed /1,4,8/. Turning over to a finite height film, the effective inplane field is composed of an external portion h_{ip} and the contribution of the domain wall stray field h_n according to Hubert /6/. Defining an effective inplane field

$$h'_{ip} = h_{ip} \cos(\varphi - \varphi_h) + h_n(z) \cos(\varphi - \varphi_n) \quad (1)$$

and an effective quality factor

$$Q' = \left(\frac{\Lambda_0}{h} \frac{d\varphi}{dz} \right)^2 + Q_1 + Q_2 \sin^2 \varphi + \cos^2(\varphi - \varphi_n) \quad (2)$$

the magnetization tilt $\vartheta_\infty(z)$ can be expressed

$$\sin \vartheta_\infty(z) \approx h'_{ip} / Q' \quad (3)$$

under the assumption $\varphi = \varphi_n = \text{const.}$

This leads to the wall energy density

$$\sigma = \frac{\sigma_0}{Q_1^{1/2}} \left\{ Q'^{1/2} \cos \vartheta_\infty(z) - \frac{\pi - 2\vartheta_\infty(z)}{2Q'^{1/2}} h'_{ip} \right\} \quad (4)$$

and the domain wall width

$$A(z) = \frac{A_0}{1 - \sin \vartheta_\infty(z)} \left(\frac{Q_1}{Q'} \right)^{1/2} \quad (5)$$

Equations of motion proposed by Slonczewski /5/ were modified by introducing the magnetization tilt in order to simply consider the influence of an inplane field /1/. Following Slonczewski's treatment and incorporating eqs. (1) to (5) the subsequent Partial Differential Equations (PDEs) are derived under the assumptions that the derivatives of $\vartheta_\infty(z)$ and $h_n(z)$ are small (dots denote time derivatives).

$$\dot{q} = \frac{\gamma A / A_0}{1 + \alpha^2} 4\pi M_s \left\{ \alpha G(t) + F(\varphi) + \left(\frac{\Lambda_0}{h} \right)^2 \left[\alpha \frac{d^2 q}{dz^2} - \frac{d^2 \varphi}{dz^2} \right] \right\} \quad (6)$$

$$\dot{\varphi} = \frac{\gamma}{1 + \alpha^2} 4\pi M_s \left\{ G(t) - \alpha F(\varphi) + \left(\frac{\Lambda_0}{h} \right)^2 \left[\frac{d^2 q}{dz^2} + \alpha \frac{d^2 \varphi}{dz^2} \right] \right\} \quad (7)$$

where

$$G(t) = h_p P(t) - h_c \text{sgn } \dot{q} \quad (8)$$

$P(t)$ represents the experimental pulse shape, h_c the coercive field, and

$$F(\varphi) = \frac{1}{2} \{ Q_2 \sin 2\varphi - \sin 2(\varphi - \varphi_n) + \frac{\pi - 2\vartheta_\infty}{\cos \vartheta_\infty} [h'_{ip} \sin(\varphi - \varphi_n) + h_n \sin(\varphi - \varphi_n)] \} \quad (9)$$

Boundary conditions are as follows:

$$\left. \frac{d\varphi}{dz} \right|_{z=0, z=1} = \left. \frac{dq}{dz} \right|_{z=0, z=1} = 0 \quad (10)$$

The time dependent solution for the equations of motion is reached by the explicitly finite difference procedure as given by Duford-Frankel /9/. Konishi's modification /10/ leads to a significant increase in computational stability. The reliability and plausibility of the solutions obtained is controlled by varying the partition of the time and space intervals respectively through comparison to steady state results.

III - EXPERIMENTAL AND NUMERICAL METHODS

The bubble rocking experiment /11/ was used to examine dynamic transitions between wall states with and without Bloch line structures. Experimental results presented here refer to sample 081#1 with composition $(Y, Gd)_3(Fe, Ga, Mn)_5O_{12}$ and following material parameters: $h = 4.3 \mu\text{m}$, $Q_1 = 10.6$, $Q_2 = -8.23$, $4\pi M_s = 164.46 \text{ G}$, $A = 1.9 \cdot 10^{-7} \text{ erg/cm}$, $\alpha = 0.01275$, $\gamma = 1.8659 \cdot 10^7 \text{ (s Oe)}^{-1}$. Local HBL-nucleation could be demonstrated at a (0,0/0)-stripe head (Fig.1d) by dynamic elongation of the stripe domain or a local inplane field acting on the stripe domain head. The rocking experiment yields the specific pulse time t_p where a dynamic state transition is observed at a fixed

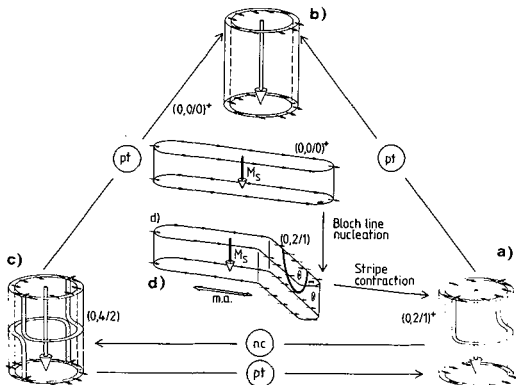


Fig. 1 Experimentally observed dynamic wall conversions
 pt: HBL-punchthrough, nc: HBL-nucleation

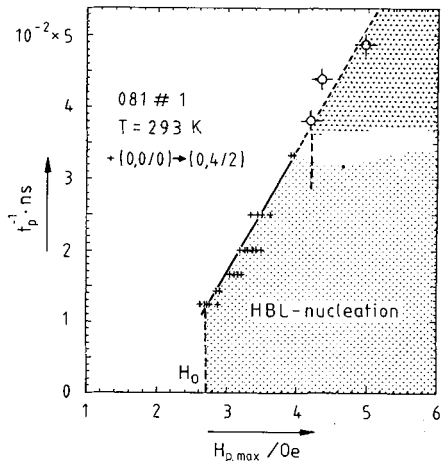


Fig. 2 Pulse time $t_p = t_{nc}$ for HBL-nucleation versus drive field $H_{p,max}$ + bubble rocking experiment
 Q: data from computer simulations

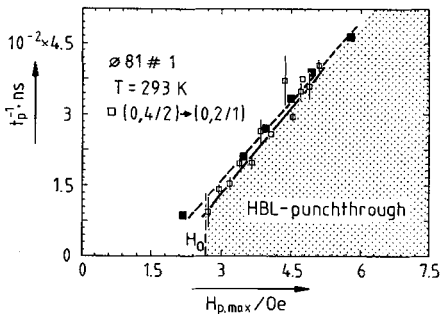


Fig. 3 Pulse time $t_p = t_{pt}$ for HBL-punchthrough versus drive field $H_{p,max}$
 □ bubble rocking experiment
 ■ computer simulations

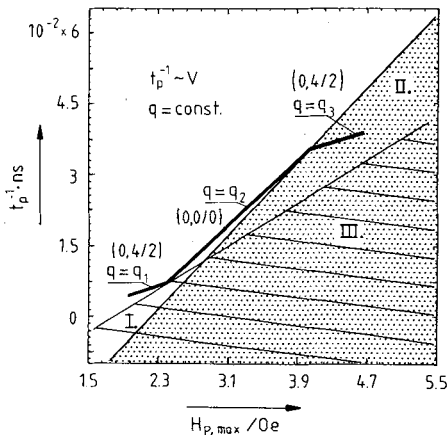


Fig. 4 Schematic dynamic stability map
 The solid lines represent translational bubble motion along different ways q .
 I. HBL-punchthrough, II. HBL-nucleation
 III. Wall oscillation

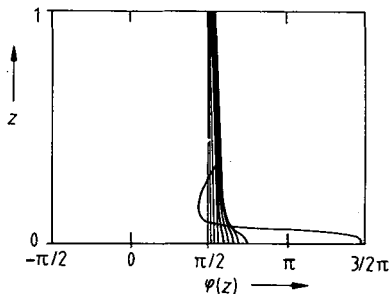
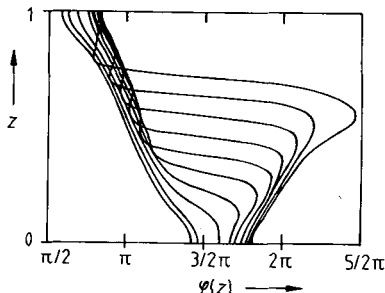


Fig. 5 Typical time resolved Bloch line nucleations (sample 081)
 a.) $Q_z = -8.23$, time step: 2.27 ns, nucleation after 28.4 ns, $\langle q_{max} \rangle = 335.3$ m/s



b.) $Q_z = 0$, time step: 2.56 ns, $\langle q_{max} \rangle = 115.59$ m/s

amplitude $H_{p,max}$. Subsequently the resultant state can be discriminated taking advantage of the well known properties of wall states in orthorhombic garnets /1/. Experimental verifications of conversions by HBL-nucleation are: $(0,0/0)^{+,-} \rightarrow (0,2/1)^{+,-}$ or $(0,0/0)^{+,-} \rightarrow (0,4/2)$ or $(0,2/1)^{+,-} \rightarrow (0,4/2)$ (Fig.1). Nucleation initiates above a threshold of the drive field $H_{p,max} = H_0$ from which point on the reciprocal pulse time $t_p^{-1} = t_{nc}^{-1}$ depends linearly on $H_{p,max}$ for $H_{p,max} > H_0$ (Fig.2). Two conversions can be attributed to HBL-punchthrough, $(0,4/2) \rightarrow (0,2/1)^{+,-}$ and $(0,4/2) \rightarrow (0,0/0)^{+,-}$ (Fig.1) and a similar linear relation can be found between $H_{p,max}$ and the pulse time $t_p = t_{pt}$ (Fig.3). As an appropriate procedure to experiments in computer simulation a moment of wall conversion is approached by successive pulse width increases with an increment $\Delta t = 1$ ns. Time development of wall momentum $\langle \dot{\phi} \rangle$ (averaged over film thickness) serves as criterion for pulse width incrementation /1/. Computer simulations firstly focus on a Néel wall and secondly on a Néel wall with HBL both moving parallel to m.a. similar to the wall states $(0,0/0)$ and $(0,2/1)^{+,-}$ or $(0,4/2)$ respectively.

IV - RESULTS AND DISCUSSION

Experimental results concerning HBL-nucleation supplemented with HBL-punchthrough data lead to a dynamic stability map (Fig.4) for stray field oriented domains and those without Bloch line structures. As main results can be stated that beyond the range of HBL stability there are new statically and dynamically stable wall states whereas Bloch line instability leads to nonlinear wall motion in films with negligible inplane anisotropy /12/. The lines in Fig.4 specify a translational motion of a bubble along a fixed distance q , i.e. a proportional relationship to domain velocity, demonstrating possible induced state conversions. Starting from $(0,4/2)$ ($q=q_1$) punchthrough takes place at the first stability boundary resulting in the state $(0,0/0)^{+,-}$. Further increase in pulse amplitude keeping the translational distance $q=q_2$ constant $(0,0/0)^{+,-}$ remains stable until the nucleation boundary is approached. At the other side of this border (Fig.4, region II, $q=q_3$) $(0,4/2)$ is found to be stable again.

Punchthrough - Comparison of experimental data with computer simulations exhibit an excellent agreement within the systematical uncertainties of simulation and experiment (Fig.3). The agreement also includes the threshold value H_0 for punchthrough onset.

Nucleation - In contrast the threshold for HBL-nucleation is significantly lower than that yielded by simulations (Fig.2) although quantitative agreement is obtained. So far simulation predicts an extended dynamic stability range of a Néel wall, corresponding to steady state approximation /4/, compared to an HBL-wall structure whereas the threshold values for dynamic instability of $(0,0/0)^{+,-}$ and $(0,4/2)$ domains are roughly identical (Fig's 2 and 3). The reason for observed HBL-nucleation at minor values of $H_{p,max}$ in experiment has not been conceived up till now.

Simulations of the Néel wall yield higher maximum velocities $v_{cr,nw}$, characterized by HBL-nucleation, for movements perpendicular to m.a. as predicted by the theory of Schlömann /13/, where the experiment shows contradictory results. Possible reasons for the quantitative discrepancies concerning HBL-nucleation might be referred to the fact that Bloch line nucleation is initialized right at the film surface in orthorhombic garnets (Fig.5a.), but more underneath the surface for films without inplane anisotropy (Fig.5b.).

The computed filmthickness dependence of $v_{cr,nw}$ exhibits a remarkable decrease with increasing (h/Λ_0) ratio, thus contradicting the experimental results of Breed /14/. Own preliminary experiments support our numerical results. The average wall mobility of the Néel wall agrees quite well with the experimental value for $(0,0/0)^{+,-}$ bubbles. A large overshoot of approx. 100 % is observed in the HBL-structure simulation, leading to a much higher average mobility compared to experimental data for the wallstate $(0,4/2)$.

REFERENCES

- /1/ Research Report No. 6, 7, and 8 of the Project No. 423-7291-NT-2576 German Ministry of Research and Technology "BMFT".
- /2/ The new notation relates to the former used ones in /1,4,8/ as follows: $(0,0/0)^{+,-} \rightarrow S = 0C^{+,-}$, $(0,2/1)^{+,-} \rightarrow S = 0C^*$, $(0,4/2) \rightarrow S = 0E$
- /3/ S.Konishi, IEEE Trans. Magn., MAG-19, (5), (1983), 1838.
- /4/ D.Krumbholz, J.Heidmann, J.Engemann and R.A.Kösinski, IEEE Trans.Magn., MAG-20, (5), (1984), 1138.
- /5/ J.C. Slonczewski, Intern. J. Magnetism, 2, (1972), 85.
- /6/ A. Hubert, J.Appl.Phys., 46, (7), (1975), 2276.
- /7/ A. Hubert, "Theorie der Domänenwände in geordneten Medien" Springer Verlag, Berlin, 1974.
- /8/ J.Heidmann, D.Krumbholz, J.Engemann, IEEE Trans.Magn., MAG-17, (6), (1981).
- /9/ J.Noye (ed.), Computational Techniques for Differential Equations, North-Holland, Amsterdam, 1984.
- /10/ S.Konishi, K.Matsuyama, I.Chida, S.Kubota, H.Kawahara, M.Ohbo, IEEE Trans. Magn., MAG-20, (5), (1984), 1129.
- /11/ G.P.Vella-Coleiro, Appl.Phys.Lett., 21, (1971), 7.
- /12/ A.P. Malozemoff, J.C. Slonczewski, "Magnetic Domain Walls In Bubble Materials", Academic Press, New York, 1979.
- /13/ Schlömann E., J.Appl.Phys., 47, (3), (1976), 1142.
- /14/ D.J. Breed, P.G.J. Nederpel, and W. de Geus, J.Appl.Phys., 54, (11), (1983), 6577.